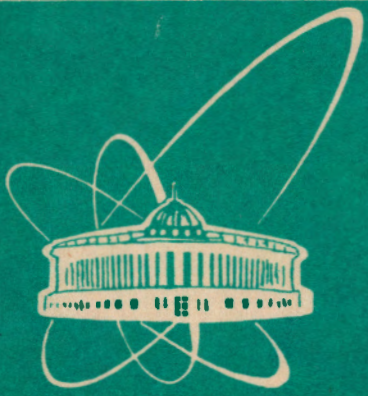

объединенный
институт
ядерных
исследований
дубна

E13-93-295

E.H.Bellamy[1], G.Bellettini[1], J.Budagov[2], F.Gervelli[1],
I.Chirikov-Zorin[3], M.Incagli[1], D.Lucchesi[1],
C.Pagliarone[1], S.Tokar[4], F.Zetti[1]

ABSOLUTE CALIBRATION AND MONITORING OF A SPECTROMETRIC CHANNEL USING A PHOTOMULTIPLIER

Submitted to «Nuclear Instruments and Methods»

[1]Dipartimento di Fisica della Universita & INFN, Pisa
[2]SSC Laboratory, Dallas. On leave from Joint Institute for Nuclear Research, Dubna, Russia
[3]Joint Institute for Nuclear Research, Dubna
[4]Comenius University, Bratislava

1993

1 Introduction

Scintillation detectors (counters, calorimeters etc.) are presently extensively used and will be used in future experiments at new accelerators. Usually in such detectors photomultiplier tubes (PM) are used for the detection of light. In detectors of this type there exists not only an intrinsic spread in characteristic parameters among different PM's, but also some time dependence of parameters of a given PM. Therefore a system of calibration and monitoring of the PM based spectrometric channels is an important part of the experimental setups employing scintillation detectors.

Particular interest is paid to the absolute calibration, i.e. to the measurement of the energy released in the scintillators in terms of the number of photoelectrons emitted from the photocathode. Usually the performances of detectors using scintillation light are qualified by this ratio, i.e. in units of photoelectrons per GeV.

The measurement of the light yield in absolute units is particularly important for research and development studies of new detectors, where it enables a direct comparison of parameters of different scintillator shapes, scitillation materials, photodetectors etc. [1,2,3].

In this work we present a method for the absolute calibration of spectrometric channels based on a statistical analysis of the PM spectra from a pulsed light source. The work was carried out in the frame of R&D programs on scintillation detectors for the CDF (Fermilab) and SDC (SSCL) collaborations.

2 A Model of Photomultiplier Response

The basic idea of the submitted calibration method consists in a deconvolution of the PM pulse height spectrum and in the use of some of the extracted parameters for calibration purposes. Hence a realistic PM response function is a very crucial point of the method. We have constructed this function according to the mode of operation of a PM [4]. The PM is treated as an instrument consisting of two independent parts:

– the photodetector where the flux of photons is converted into electrons;

– the amplifier (dynode system), which amplifies the initial charge emitted by the photocathode.

Therefore the operation for a PM can be devided into two independent processes: photoconversion and electron collections, and amplification.

2.1 Photoconversion and Electron Collection

Let us suppose that we have a pulsed source of light (in practice we used a light emission diode (LED)). The flux of photons incident on the PM photocathode produces photoelectrons via the photoelectric effect. Under a real circumstances the number of photons hitting the photocathode is not a constant but Poisson distributed variable. This follows from the fact that only a fraction of the incident photons is picked up by the PM. The conversion of photons into electrons and their subsequent collection by the dynode system is a random binary process. Therefore the distribution of number of photoelectrons can be expressed as a convolution of Poisson and binary processes. This gives again a Poisson distribution:

$$P(n;\mu) = \frac{\mu^n e^{-\mu}}{n!} \tag{1}$$

with μ defined as

$$\mu = mq \tag{2}$$

where:

- μ - the mean number of photoelectrons collected by the first dynode.
- $P(n;\mu)$ - the probability that n photoelectrons will be observed at the PM output when their mean is μ;
- m - the mean number of photons hitting the photocathode;
- q - the quantum efficiency of photocathode.

We would like to note that μ is a parameter characterizing not only the light source intensity but also the photocathode quantum efficiency and the electron collection efficiency of the PM's dynode system. Thus μ, the mean number of collected photoelectrons, is determined by the mean number of photons hitting the photocathode, the photocathode quantum efficiency, and the collection efficiency of the dynode system.

2.2 Amplification

The response of a multiplicative dynode system to a single photoelectron, when the coefficient of secondary electron emission by the first dynode is large (> 4) and the coefficient of secondary electron collection by the first few dynodes is close to one, can be approximated by a Gaussian distribution:

$$G_1(x) = \frac{1}{\sigma_1\sqrt{2\pi}} exp\left(-\frac{(x-Q_1)^2}{2\sigma_1^2}\right) \tag{3}$$

where:

- x is the variable charge;
- Q_1 is the average charge at the PM output when one electron is collected by the first dynode;
- σ_1 is the corresponding standard deviation of the charge distribution.

Of course Q_1 can be expressed through the PM gain coefficient g and elementary charge e, as $Q_1 = e\,g$.

The PM output charge distribution when more than one photoelectron are collected by the first dynode can be derived from formula (3) if one assumes that the amplification processes of the charges initiated by different photoelectrons are mutually independent. In this case the charge distribution when the process is initiated by n photoelectrons, is a convolution of n one-electron cases:

$$G_n(x) = \frac{1}{\sigma_1\sqrt{2\pi n}} exp\left(-\frac{(x-nQ_1)^2}{2n\sigma_1^2}\right) \tag{4}$$

Note that this distribution has the correct limit for $n \to 0$:

$$G_0(x) = \delta(x)$$

where $\delta(x)$ is the delta function. This condition ensures that the amplification of an input zero charge results in zero charge at the output.

It is important to note that expression (4) is correct provided the chance of a photoelectron missing the first dynode and being captured by one of the subsequent dynodes is negligible.

The response of an ideal noiseless PM can now be readily found. In this case the resulting output signal is simply a convolution of the distributions (1) and (4):

$$S_{ideal}(x) = P(n;\mu) \otimes G_n(x) = \sum_{n=0}^{\infty} \frac{\mu^n e^{-\mu}}{n!} \frac{1}{\sigma_1 \sqrt{2\pi n}} exp\left(-\frac{(x - nQ_1)^2}{2n\sigma_1^2}\right) \quad (5)$$

With the above mentioned limit condition for n=0.

2.3 Background Processes

In a real PM, in addition to the process of conversion of light and subsequent amplification of charge, various background processes will always be present which will ultimately generate some additional charge (noise). Such noise signals in the anode circuit could be generated even in the absence of a light signal. An additional component of noise is generated in the presence of light.

The possible noise sources are: thermoelectron emission from the photocathode and/or the dynode system; leakage current in the PM anode circuit; electron autoemission by electrodes; photon and ion feedbacks; external and internal radioactivity etc.

Spurious signals of small amplitude can also arise at the PM output which are due to the incident photon flux. Possible sources of these signals are: photoemission from the the focusing electrodes and dynodes, photoelectron missing the first dynode end, etc. One can expect the amplitude of these signals to decrease approximately exponentially, and therefore we will consider these signals as a noise.

The background processes generate an additional charge and modify the output charge spectrum. The resulting spectrum is a convolution of the ideal PM spectrum (5) with the background charge distribution. We shall split the background processes into two groups with different distribution functions:

– (I) the low charge processes present in each event (e.g. the leakage current etc.) which are responsible for non-zero width of the signal distribution when no photoelectron was emited from photocathode ("Pedestal");

– (II) the discrete processes which can with non-zero probability accompany the measured signal (such as thermoemission, noise initiated by the measured light, etc.).

The processes of type I can be described by a Gaussian and those of type II by an exponential function.

The effect of these processes when some primary photoelectrons ($n \geq 1$) are emitted will be discussed later. When no primary photoelectron is emitted (n=0, with probability $e^{-\mu}$), the totality of the signal will be due to these backgrounds. If we call w the probability that, within these events, a background signal of type II can occur, we can parameterize the background as:

$$B(x) = \frac{(1-w)}{\sigma_0\sqrt{2\pi}}\, exp\left(-\frac{x^2}{2\sigma_0^2}\right) + w\,\theta(x)\,\alpha\, exp(-\alpha x) \qquad (6)$$

where:

σ_0 is the standard deviation of the type I background distribution;

w is the probability that a measured signal is accompanied by a type II background process.

α is the coefficient of the exponential decrease of type II background;

$\theta(x) = \begin{cases} 0 & x < 0 \\ 1 & x \geq 0 \end{cases}$ is the step function.

The first term in (6) corresponds to the situation when only the low charge background processes are present. The second term corresponds to the presence of both groups of background. For small σ_0 ($\ll 1/\alpha$) the convolution of a Gaussian with an exponential function is reduced to a pure exponential function.

2.4 The Realistic Response Function of the PM

Taking into account the ideal PM spectrum (5) and the background charge distribution (6) we find the realistic PM spectrum as the convolution:

$$S_{real}(x) = \int S_{ideal}(x')B(x-x')dx' =$$

$$= \sum_{n=0}^{\infty} \frac{\mu^n e^{-\mu}}{n!}[(1-w)\,G_n(x-Q_0) + w\,I_{G_n \otimes E}(x-Q_0)] \qquad (7)$$

$$I_{G_n \otimes E}(x-Q_0) = \int_{Q_0}^{x} G_n(x'-Q_0)\,\alpha\,exp[-\alpha(x-x')]dx' =$$

$$= \frac{\alpha}{2}\,exp[-\alpha(x-Q_n-\alpha\,\sigma_n^2)]\times$$

$$\times \left[erf\left(\frac{|Q_0-Q_n-\sigma_n^2\alpha|}{\sigma_n\sqrt{2}}\right) + sign(x-Q_n-\sigma_n^2\alpha)\,erf\left(\frac{|x-Q_n-\sigma_n^2\alpha|}{\sigma_n\sqrt{2}}\right)\right] \qquad (8)$$

$$Q_n = Q_0 + nQ_1$$

$$\sigma_n = \sqrt{\sigma_0^2 + n\sigma_1^2} \approx \begin{cases} \sigma_0 & n = 0 \\ \sqrt{n}\sigma_1 & n > 0 \end{cases}$$

where Q_0 is the pedestal and $erf(x)$ is the error function.

The meaning of the other parameters is the same as in (1), (4) and (6). $G_n(x)$ is now a convolution of the ideal PM n photoelectrons charge distribution (5) with the Gaussian part of background (6). The standard deviation connected with $G_n(x)$ is $\sqrt{\sigma_0^2 + n\sigma_1^2}$. In practical cases ($\sigma_0 \ll \sigma_1$) for a non-zero photoelectron number the ideal PM standard deviation ($\sigma_1\sqrt{n}$) can be used. In the zero photoelectron case $G_0(x-Q_0)$ is not a delta function any more, but a Gaussian with standard deviation σ_0. Hence, $I_{G_n \otimes E}$ is reduced to $\alpha\,exp[-\alpha(x-Q_0)]$.

As a conclusion we would like to note that the response function (7) of a real PM contains 7 free parameters. Two of them (Q_0 and σ_0) define the

pedestal. Two other ones, w and α describe the discrete background, and the remaining 3 parameters (Q_1, σ_1 and μ) describe the spectrum of the real signal . Of these 3 parameters one (μ) is proportional to the intensity of the light source and two remaining ones (Q_1 and σ_1) characterize the amplification process of the PM dynode system.

The fact that the intensity of the light source can be separated from the amplification process plays a crucial role in the calibration and monitoring of a spectrometric channel. If we are able to deconvolute the spectrum indicated in (7), i.e. to find its parameters, we can use parameter Q_1 as a calibration unit as well as a parameter for checking the stability of PM operation. The absolute PM gain coefficient is also given by Q_1 . The stability of the photoelectron signal will be monitored by μ.

2.5 Approximating the PM Response Function

The PM response function (7) is relatively complicated to be treated as a fitting function and in some cases useful approximations to it can be found. If the noise intensity is low ($1/\alpha << Q_1$) and μ is large (≥ 2) then, for the non-pedestal part of spectrum, we can treat the background as some effective additional constant charge shifting the spectrum. Mathematically this means that for $n \geq 1$ in formula (7) we would use as the background function:

$$B(x) = \frac{1}{\sigma_0\sqrt{2\pi}}\, exp\left(-\frac{(x - Q_0 - Q_{sh})^2}{2\sigma_0^2}\right) \tag{9}$$

instead of (6). In this case, the PM response function is:

$$S_{real}(x) \approx \left\{\frac{(1-w)}{\sigma_0\sqrt{2\pi}} exp\left(-\frac{(x-Q_0)^2}{2\sigma_0^2}\right) + w\theta(x - Q_0)\alpha exp[-\alpha(x - Q_0)]\right\}e^{-\mu} +$$

$$+ \sum_{n=1}^{\infty} \frac{\mu^n e^{-\mu}}{n!} \frac{1}{\sigma_1\sqrt{2\pi n}}\, exp\left(-\frac{(x - Q_0 - Q_{sh} - nQ_1)^2}{2n\sigma_1^2}\right) \tag{10}$$

$$Q_{sh} = w/\alpha \tag{11}$$

where Q_{sh} is the effective spectrum shift due to background.

2.6 The Large μ Case

It is important to consider the limit of (7) for high intensity sources. At large μ the Poisson distribution goes over to a Gaussian, with standard deviation $\sqrt{\mu}$ and of all G_n functions, only those with $\mu - \sqrt{\mu} < n < \mu + \sqrt{\mu}$ will effectively contribute. Practically, this means that for large μ we can approximate the standard deviation of G_n ($\sigma_1\sqrt{n}$) by $\sigma_1\sqrt{\mu}$.

Therefore replacing $\sum_n \ldots \rightarrow \int dn \ldots$ and treating the charge generated by the background processes effectively via Q_{sh} (11) we will find for the limit spectrum:

$$S_\infty(x) = \frac{1}{\sqrt{2\pi\mu(\sigma_1^2 + Q_1^2)}} exp\left(-\frac{(x - Q_0 - Q_{sh} - \mu Q_1)^2}{2\mu(\sigma_1^2 + Q_1^2)}\right) \qquad (12)$$

$S_\infty(x)$ is Gaussian and therefore has only two free parameters. In the limit case the three parameters μ, Q_1 and σ_1 are not independent:

$$Q_\infty = \mu Q_1 \qquad (13)$$

$$\sigma_\infty = \sqrt{\mu(\sigma_1^2 + Q_1^2)} \qquad (14)$$

Q_0 is the pedestal and should be treated separately. We note that in this limit we cannot separate the light source intensity (μ) from the PM amplification (Q_1).

2.7 Conclusion

The model that we have developed is applicable to PM's with large (> 4) coefficient of secondary emission on the first dynode, when the collection coefficient of the first few dynodes is close to 1. These requirements are met by many modern PM's. The model can be made applicable for any PM if the Poisson fluctuation in the number of secondary electrons on the first few dynodes, and the coefficients for electron collection are taken into account.

3 Example of an Application of the Method

The developed analytical method was applied to the calibration of a few PM's employing a low intensity pulsed light source [6]. The block diagram for the calibration measurement is shown in Fig. 1. A LED was used as

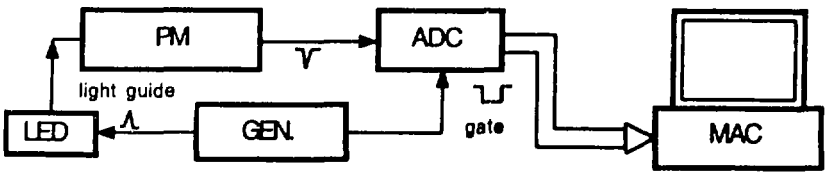

Fig. 1 Block scheme of the calibration setup.

a pulsed light source. The LED was driven by a pulse generator (GEN) with a short pulse width ($\leq$ 10 ns). An optical fiber was used to transmit light from the LED to the PM so as to eliminate electrical noise from the generator.

The photon intensity incident the photocathode was tuned by changing the amplitude of the supply voltage to the LED.

The analog output signal from the PM was measured by an ADC (LeCroy 2249A). The width of the gate signal was 80 ns. The output information from the ADC was read by means of a Macintosh II computer.

4 LED Spectra

In order to apply and test our calibration and monitoring method based on a deconvolution of the LED spectrum, we carried out a series of LED spectra measurements. The measurements differed in light source intensity, applied voltage to PM, as well as in the type of PM used.

Most of measurements were carried out using an EMI-9814B photomultiplier. Some spectra were also taken with an XP1910 and FEU184 (produced by MELZ, Moscow).

Pulse height spectra were deconvoluted by means of a program based on the Minuit Minimization Package using the PM response function (7) as fitting function.

The results of spectral processing are summarized in the figures and in the tables presented below.

A typical deconvoluted LED spectrum is presented in Fig. 2. It corresponds to an average of 1.7 photoelectrons collected from the PM photocathode. The solid line corresponds to the PM response function (7), with fitted parameters as given in the figure. The dashed curves represent the background and partial charge distributions corresponding to $n = 1, 2, 3...$ photoelectrons emitted by the photocathode. The maximal number of photoelectrons handled by the fitting procedure varied from 9 ($\mu < 2$) to 15 for large μ (4). The asymmetry of the partial charge distributions is caused by the convolution of the ideal distributions with background and decreases with increasing n. From Fig. 2 we see that the experimental spectrum is fitted well and the parameter $Q_1(channel/ph.e.)$ we are interested in is

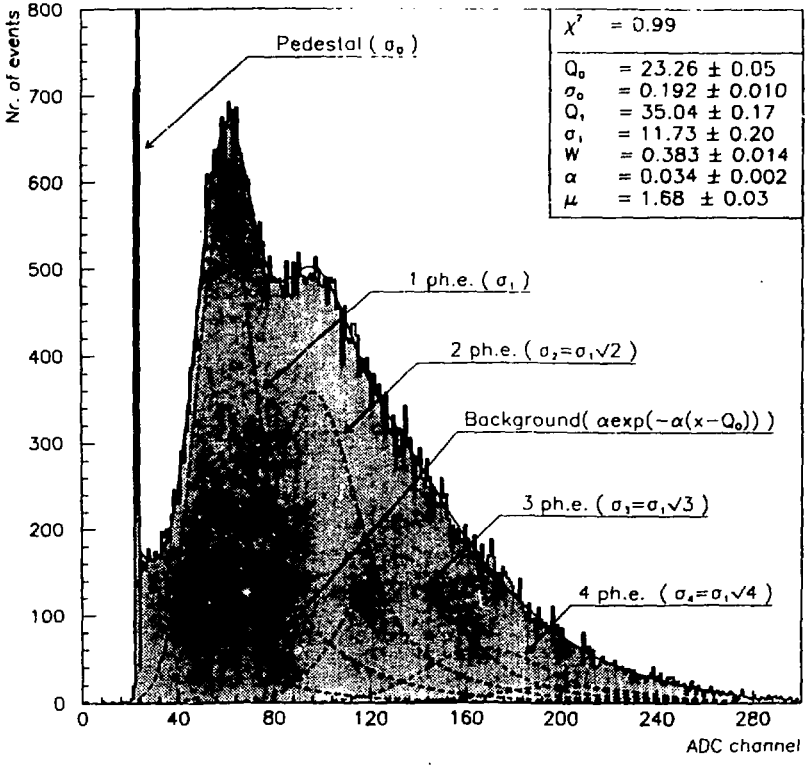

Fig. 2 Typical deconvoluted LED spectrum (EMI - 9814B photomultiplier).

defined with high accuracy (< 1%). The parameter errors were found by Minuit Minos analysis [5].

We have also checked the stability of the deconvolution procedure and studied the range of applicability of the method. For this purpose we carried out another series of measurements changing the input light signal. Some spectra were taken even at the same level of input signal. The measurements were carried out during a short time period, therefore drift in apparatus parameters should not be significant. The results of the deconvolution analysis of the measured spectra are presented in Table 1 and in Figs. 3a - 3h.

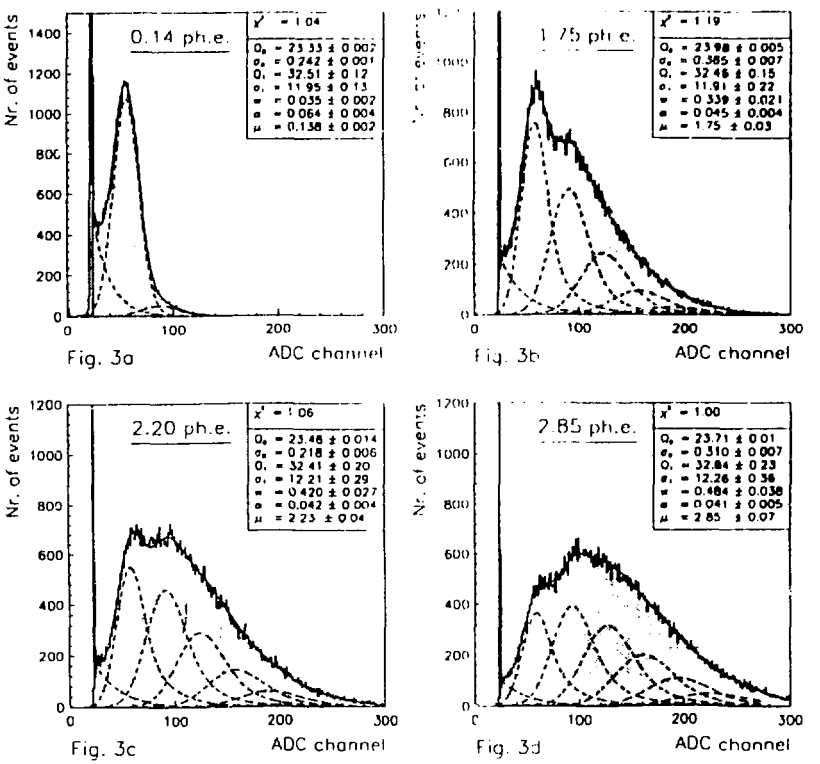

Fig. 3 LED spectra taken with a EMI-9814B photomultiplier constant voltage for different intensity of light source (0.1 - 6.7 photoelectrons).

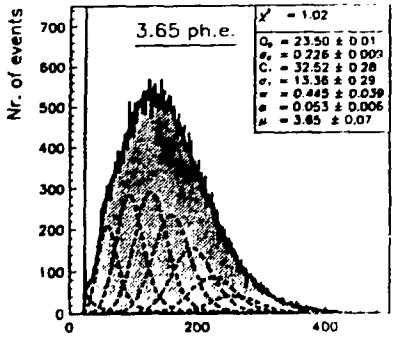

Fig. 3e

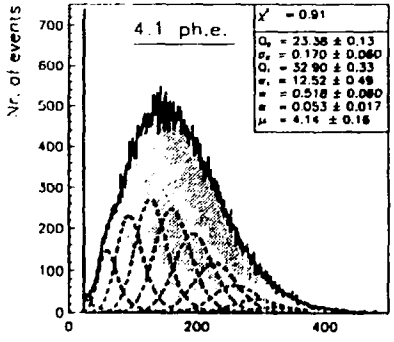

Fig. 3f

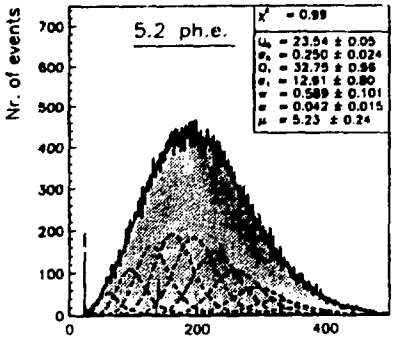

Fig. 3g

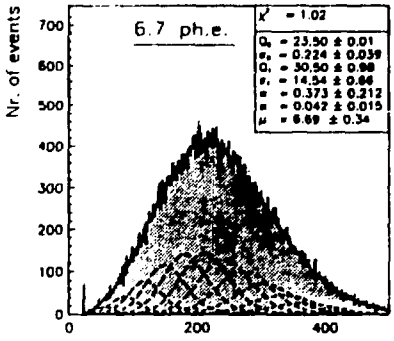

Fig. 3h

The results demonstrate good stability of the deconvolution procedure for a wide range of input light intensity μ, from 0.1 to ~ 5 photoelectrons. The parameter errors for the spectra with large light input (e.g. Fig. 3h, $\mu = 6.7$) tend to increase and the correlations among the parameters μ, Q_1 and σ_1 become substantial. Because of these correlations it is recommended to use for calibration a low intensity source (< 3 ph.e.).

Deconvolution of sources with small μ (< 0.5 ph.e.) is possible, (as can be seen from Table 1 and Fig. 3a) but, because of the large number of pedestal events, high statistics must be taken.

From Table 1 we can also note an increasing probability for PM background (w) with increasing light intensity. This tendency is not surprising, since the increasing number of photons hitting the focusing electrodes and the dynode system will produce more background.

To check the flexibility of the method we applied it to spectra of different PM's and different PM regimes. Pulse height spectra were deconvoluted as before and the corresponding results are summarized in Figs. 4a - 4d.

The first two spectra were taken with two different EMI-9814B PM's. The next two spectra were measured with an XP1910 (Fig. 4c) and a FEU184 (Fig. 4d).

In the figures we present the deconvolution parameters as well as the PM single electron resolution, $\delta = \sigma_1/Q_1(\%)$. The gain coefficient was obtained

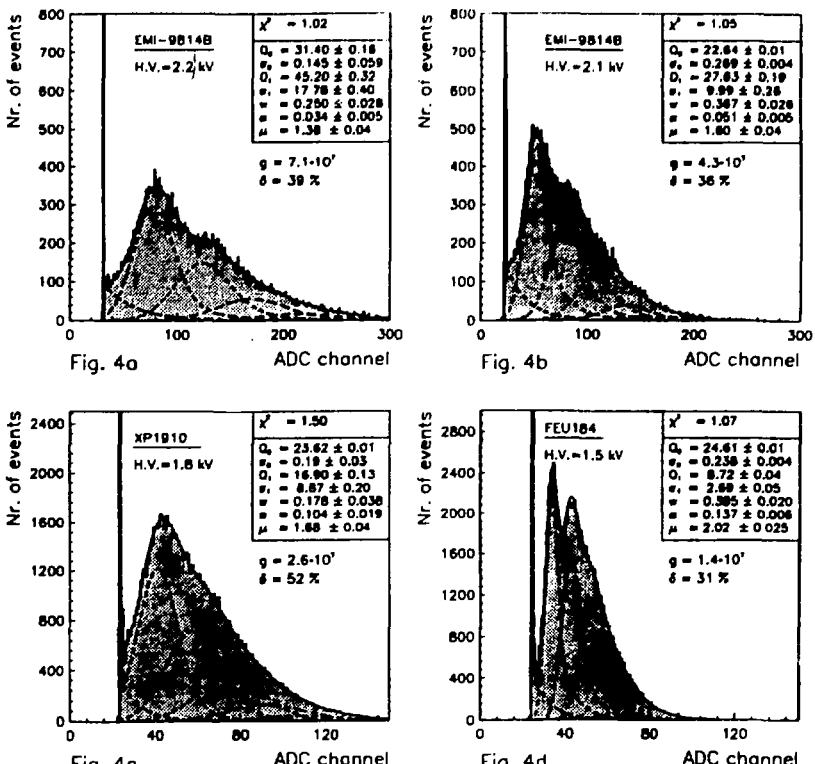

Fig. 4 LED spectra taken with different photomultipliers (EMI - 9814B, XP1910 and FEU184).

using the Q_1 parameter and the ADC channel width ($0.25pC/channel$) as

$$g = Q_1 \frac{2.5 \times 10^{-13}C}{1.602 \times 10^{-19}C} \tag{15}$$

As can be seen from Fig. 4a - 4d, all spectra are deconvoluted satisfactorily. The relatively bad χ^2 for the PX1910 can probably be explained by it's poor coefficient of secondary emission on the first dynode. In this case Poisson fluctuations in the first dynode would have to be taken into account for the correct description of the spectrum.

For the use of Q_1 as a calibration means it is important to have optimal statistics. In principle, the accuracy of the spectral parameters increasing with statistics. On the other hand, if the statistics of one channel in the spectrum maximum (out of pedestal) is higher than about 600 counts per channel, the error generated by the differential non-linearity of our ADC would have dominated over the statistical error.

To keep the accuracy of the Q_1 parameter better than 1%, one should take about 50,000 - 100,000 events per spectrum provided that the source intensity is between 0.5 and 2.5 photoelectrons.

5 Conclusions

A method for calibrating and monitoring a PM based spectrometer using a deconvolution of the PM spectra was developed.

The adopted PM response function contains 7 free parameters, whose physical interpretation is simple and clear.

The parameter used for calibration (light detector gain) can be obtained with a precision of about 1%.

The light source intensity and PM gain are monitored by different parameters. This allows the light intensity to be changed from one measurement to another provided that it is stable during each measurement. However, it should be noted that the photocathode efficiency cannot be extracted in the frame of this method.

The method can be useful in a number of applications:

1) research and development of scintillation fiber and tile calorimeters the study of light output from individual tiles;

2) the investigation of performances of counters employing scintillator bars (e.g. muon trigger counters) [7];

3) the study of single electron response, gain, noise and other characteristics of photomultipliers.

In conclusion we would like to emphasize that this method can be employed not only in spectrometric channels using PM's, but also for other types of photodetectors.

Table 1 Parameters of LED spectra taken with an EMI - 9814B photomultiplier at constant voltage for different intensity of light source (0.1 : 6.7 photoelectrons).

Table 1: LED spectra at different light source intensities						
μ	Q_0	σ_0	Q_1	σ_1	w	$\alpha\,(10^{-1})$
0.14	23.33	0.24	32.51	11.95	0.035	0.64
± 0.002	± 0.01	± 0.01	± 0.12	± 0.13	± 0.002	± 0.02
1.72	23.94	0.39	32.36	11.87	0.35	0.40
± 0.03	± 0.01	± 0.01	± 0.15	± 0.21	± 0.02	± 0.02
1.75	23.98	0.39	32.46	11.91	0.34	0.45
± 0.03	± 0.01	± 0.01	± 0.15	± 0.22	± 0.02	± 0.03
1.73	24.00	0.39	32.35	12.07	0.34	0.43
± 0.03	± 0.01	± 0.01	± 0.15	± 0.22	± 0.02	± 0.03
2.23	23.48	0.22	32.41	12.22	0.42	0.42
± 0.04	± 0.01	± 0.01	± 0.20	± 0.29	± 0.03	± 0.03
2.59	23.50	0.22	32.52	12.52	0.40	0.47
± 0.07	± 0.01	± 0.01	± 0.20	± 0.34	± 0.04	± 0.08
2.85	23.71	0.31	32.84	12.26	0.48	0.41
± 0.07	± 0.01	± 0.01	± 0.23	± 0.36	± 0.04	± 0.05
3.65	23.50	0.22	32.52	13.36	0.45	0.53
± 0.07	± 0.01	± 0.01	± 0.29	± 0.29	± 0.04	± 0.05
4.14	23.38	0.17	32.90	12.52	0.52	0.53
± 0.16	± 0.13	± 0.06	± 0.20	± 0.49	± 0.08	± 0.17
5.25	23.55	0.25	32.54	13.08	0.60	0.42
± 0.25	± 0.05	± 0.02	± 0.55	± 0.83	± 0.10	± 0.13
6.70	23.50	0.22	30.50	14.54	0.37	0.42
± 0.34	± 0.01	± 0.04	± 0.98	± 0.66	± 0.21	± 0.15

6 Acknowledgement

The authors want to thank to Prof. Giuseppe Pierazzini, Director of INFN Pisa, and Prof. A.N. Sissakian for their continuous support. Thanks are also due to Dr. D. O'Connor of Honolulu University for an accurate reading of the manuscript and for valuable remarks.

References

[1] M.Bott-Bodenhausen et al., NIM A315(1992) 236-251

[2] P.de Barbaro et al., NIM A315(1992) 317-321

[3] B.Bencheikh et al., NIM A315(1992) 349-353

[4] Ralph W. Engstrom, Photomultiplier Handbook (Lancaster, PA, USA: RCA, Solid State DIvision, 1980)

[5] MINUIT Minimization and Error Analysis, Release 89.12j, CERN, Geneva 1989.

[6] G.Bellettini et al., JINR Preprint **E13-93-296**, Dubna, 1993.

[7] Solenoidal Detector Collaboration, 4S Technical Design Report, SDC-92-201, 1 April 1992.

Received by Publishing Department
on July 29, 1993.